Title

Accounting for the effects of buoyancy on the turbulent scalar fluxes

Journal

Environmental Fluid Mechanics, 19(2)

ISSN

1567-7419

Authors

Younis, Bassam A
Jooß, Yannik
Spring, Sebastian
et al.

Publication Date

2019-04-01

DOI

10.1007/s10652-018-9635-3

Peer reviewed

Environmental Fluid Mechanics
https://doi.org/10.1007/s10652-018-9635-3

ORIGINAL ARTICLE

Accounting for the effects of buoyancy on the turbulent scalar fluxes

Bassam A. Younis[1] · Yannik Jooß[2] · Sebastian Spring[2] · Bernhard Weigand[2]

Received: 19 May 2018 / Accepted: 24 September 2018

Abstract
The paper reports on the development of an explicit, algebraic model for the turbulent scalar fluxes which properly reflects the dependence of these fluxes on the gradients of mean velocity and on gravitational acceleration. Such dependencies are required by the exact equations governing the conservation of the turbulent fluxes but are absent from models which are based on the notion of eddy diffusivity and constant Prandtl or Schmidt number. In the present contribution, tensor representation theory is used to express the scalar fluxes in terms of its vector and tensor dependencies and then by applying a few assumptions to arrive at a model that includes the proper dependencies while being sufficiently compact and robust to be of use in practical applications. Model calibration was accomplished by reference solely to data from Large-Eddy Simulations of homogeneous turbulence in neutral and stable stratification while model performance was assessed by comparisons with experimental data from two-dimensional heated plane and free jets and buoyant plumes. In all cases, the model's performance was found to be better than an alternative implicit algebraic model, and on par with that of a differential scalar-flux transport closure.

Keywords Scalar flux modeling · Buoyant flows · Stable stratification · Turbulence closure

List of symbols

C_n	Model constants (−)
G_{ij}	Rate of production of $\overline{u_i u_j}$ by buoyancy (m^2/s^3)
g_i	Gravitational acceleration (m/s^2)
k	Turbulence kinetic energy (m^2/s^2)
P_{ij}	Rate of production of $\overline{u_i u_j}$ by shear (m/s^3)
p	Pressure (Pa)
p'	Fluctuating pressure (Pa)
$P_{i\theta,1}$	Production of $-\overline{u_i\theta}$ by mean shear (m^2/s^3)
$P_{i\theta,2}$	Production of $-\overline{u_i\theta}$ by scalar gradients (m^2/s^3)
$P_{i\theta,3}$	Production of $-\overline{u_i\theta}$ by gravitational body force (m^2/s^3)
Pr	Prandtl number (−)

✉ Bassam A. Younis
bayounis@ucdavis.edu

[1] Department of Civil and Environmental Engineering, University of California, Davis, CA, USA

[2] Institut für Thermodynamik der Luft- und Raumfahrt, Universität Stuttgart, Stuttgart, Germany

Published online: 06 October 2018

Ri Gradient Richardson number (−)
Ri_{cr} Critical gradient Richardson number (−)
Re Reynolds number (−)
Re_t Turbulent Reynolds number (−)
S_{ij} Mean rate-of-strain tensor (1/s)
St Shear time (−)
t Time (s)
U_i Mean velocity component (m/s)
u_i Fluctuating velocity component (m/s)
$\overline{u_i u_j}$ Reynolds stress tensor (m^2/s^2)
$\overline{u_i \theta}$ Turbulent heat flux (mK/s)
W_{ij} Vorticity tensor (1/s)
x_i Spatial coordinate (m)

Greek letters

α Model coefficient
β Volumetric thermal expansion coefficient (1/K)
δ_θ Half width of thermal layer (m)
ϵ Dissipation rate of turbulence kinetic energy (m^2/s^3)
γ Thermal diffusivity (m^2/s)
Γ_t Turbulent (eddy) diffusivity (m^2/s)
δ_{ij} Kronecker delta (−)
θ Fluctuating temperature (K)
$\overline{\theta^2}$ Temperature variance (K^2)
Θ Mean temperature (K)
ν Kinematic viscosity (m^2/s)
ρ Density (kg/m^3)
σ_t Turbulent Prandtl number (−)
τ_{ij} Reynolds stress tensor (m^2/s^2)

1 Introduction

Accounting for the effects of buoyancy on the turbulent transport of contaminants in the atmospheric and aquatic environments is arguably amongst the most important and most difficult aspect of the computational modeling of such flows. Buoyancy-related terms that represent these effects appear explicitly in the exact differential transport equations governing the conservation of the momentum fluxes (the Reynolds stresses) and the fluxes of heat or concentration (hereafter the turbulent scalar fluxes) and hence models based on the solution of these equations have shown considerable success in capturing the influence of buoyancy on the rate of spread of shear layers, and on the rate of dilution of contaminants [1]. As these models require considerable computational effort (in three-dimensional flows, the solution of 11 differential transport equations consisting of 6 equations for the components of the Reynolds-stress tensor, 3 equations for the components of the turbulent scalar fluxes, an equation for the dissipation rate of the turbulence kinetic energy, and one for the scalar variance), considerable efforts have been directed towards the formulation of models consisting of algebraic expressions from which the Reynolds stresses and the turbulent scalar fluxes can be obtained (e.g. [2, 3]). A desirable feature in an algebraic

model is that it should be explicit in the turbulent scalar fluxes. The designation *explicit* is used in this work to describe a model wherein the flux component in a particular direction can be obtained directly from an equation that does not contain the flux components in the other two directions (contrast Eqs. 8 and 10 in the next section). Both explicit and implicit models will by necessity depend on turbulence parameters (such as the turbulence kinetic energy k and its rate of dissipation ϵ) which, in buoyant flows, will themselves depend on the scalar fluxes. Thus iterations would be required, but their purpose now would be to procure solutions that simultaneously satisfy the coupled sets of equations for the scalar fluxes and the turbulence parameters. Another desirable feature in the algebraic model is for it to be consistent with the exact differential equations governing the conservation of these fluxes. Specifically, and as will be shown in the next section, a consistent algebraic model for the turbulent scalar fluxes is one which provides for the fluxes to depend on the gradients of the scalar being transport and, in addition, on both the gradients of mean velocity and on the gravitational acceleration [4]. Such dependencies are not present in many of the models used for the computation of turbulent buoyant flows such as, for example, the gradient-transport models represented by Fourier's and Fick's laws for the turbulent heat and mass fluxes respectively:

$$-\overline{u_i\theta} = \Gamma_t \frac{\partial \Theta}{\partial x_i} \tag{1}$$

where Θ represents temperature or mass concentration, $\overline{u_i\theta}$ the turbulent fluxes and Γ_t is the eddy diffusivity which is typically related to the eddy viscosity via a relationship of the form:

$$\Gamma_t = \frac{C_\mu}{\sigma_t}\frac{k^2}{\epsilon} \tag{2}$$

where k and ϵ are, respectively, the turbulent kinetic energy and its dissipation rate and σ_t is the turbulent Prandtl or Schmidt number.

Clearly, these models, while correctly reflecting the dependence on the gradients of the scalar, do not include dependence on the gravitational acceleration or on the velocity gradients. Alternative models to Eq. (1) that do allow for the scalar fluxes to depend on these parameters have been reported in the literature, many being formulated by first modeling the unknown correlations in the exact equations for the turbulent fluxes (Eq. 3) and then by introducing assumptions that neglect the advection and diffusion of the Reynolds stresses and the scalar fluxes [5] to reduce the differential equations to algebraic ones [6]. While these models have produced distinct improvements in the prediction of some buoyant flows, they are not explicit in the turbulent fluxes and hence their implementation in numerical simulation algorithms requires that iterations are performed to obtain values of the scalar fluxes that satisfy the coupled, non-linear equations. Such iterations, in which extensive underrelaxation is employed to prevent oscillations, add considerably to the overall computational effort and this may explain the limited use of such models in practice. On the other hand, many of the recent algebraic models that are explicit in the scalar fluxes and that have been shown to work well in highly-idealized buoyant flows (e.g. [7–9]) suffer their own drawbacks when employed in the calculation of practically-relevant buoyant flows. These arise from the fact that, in non-trivial flows, these models, formulated by an approach involving a linear expansion of tensors [10] give rise to a coupled system of polynomials the solution of which renders the use of these models impractical [11]. The present contribution provides a proposal for a model for the turbulent scalar fluxes that is both

consistent with the exact equations and is explicit in these fluxes. The validity of this model is demonstrated by comparisons with data from Large-Eddy Simulations and experiments on stably-stratified flows.

2 Model development

2.1 Deductions from the exact equations

We begin by consideration of the exact equations governing the conservation of the turbulent scalar fluxes in buoyant flows. These are obtained by multiplying the u_i fluctuating velocity component by the equation for the instantaneous scalar $(\Theta + \theta)$ and add it to the x_i -component of the instantaneous Navier-Stokes equations multiplied by θ and then by time-averaging the result to obtain:

$$\overbrace{\frac{\partial(\overline{u_i\theta})}{\partial t} + U_k\frac{\partial(\overline{u_i\theta})}{\partial x_k}}^{C_{i\theta}} = \overbrace{\frac{\partial}{\partial x_k}\left(-\overline{u_k u_i\theta} - \frac{\overline{p'\theta}}{\rho}\delta_{ik} + \gamma u_i\overline{\frac{\partial\theta}{\partial x_k}} + \nu\theta\overline{\frac{\partial u_i}{\partial x_k}}\right)}^{D_{i\theta}} \overbrace{-\overline{u_k\theta}\frac{\partial U_i}{\partial x_k}}^{P_{i\theta,1}} \overbrace{-\overline{u_k u_i}\frac{\partial\Theta}{\partial x_k}}^{P_{i\theta,2}} \overbrace{-\beta g_i\overline{\theta^2}}^{P_{i\theta,3}} \overbrace{-(\gamma+\nu)\overline{\frac{\partial\theta}{\partial x_k}\frac{\partial u_i}{\partial x_k}}}^{\epsilon_{i\theta}} \overbrace{-\overline{\frac{p'}{\rho}\frac{\partial\theta}{\partial x_i}}}^{\pi_{i\theta}} \tag{3}$$

In Eq. (3), the terms $C_{i\theta}$ represent the advection of $\overline{u_i\theta}$ and $D_{i\theta}$ is the rate of transport (diffusion) of $\overline{u_i\theta}$ by turbulent processes. The terms $P_{i\theta}$ represent the rates of production of $\overline{u_i\theta}$ by interaction with the mean shear, by gradients of the scalar quantity itself, and by buoyancy. The terms $\epsilon_{i\theta}$ and $\pi_{i\theta}$ represent, respectively, the rates of dissipation by molecular processes, and of interactions with the fluctuating pressure field.

In developing an algebraic model for $\overline{u_i\theta}$, we proceed to express these correlations in terms of parameters obtained in Eq. (3):

$$-\overline{u_i\theta} = f\left(\overline{u_j u_k}, \frac{\partial U_j}{\partial x_k}, \frac{\partial\Theta}{\partial x_k}, g_i, \overline{\theta^2}\right) \tag{4}$$

By retaining the Reynolds stresses, a direct link is established between the details of the turbulence field and the turbulent scalar fluxes. It is noted that the Reynolds stresses are very sensitive to the effects of buoyancy viz. the case of strong stabilizing stratification when the turbulent shear stress vanishes at a critical value of Richardson number [12, 13]. Another reason for retaining this dependence is that the trace of the Reynolds stresses is the turbulent kinetic energy ($k \equiv 1/2\overline{u_i u_i}$) - a scalar quantity that is convenient to characterize the velocity scale of turbulence. The gradients of mean velocity are retained so that changes

in the mean velocity field are directly reflected in the turbulent scalar fluxes. It should also be useful to retain this term in the case of buoyant flows developing over a curved surface since the extra rates of strain associated with streamline curvature that are essential for the accurate prediction of these flows emerge directly from this term [14, 15]. Retention of gradients of the scalar Θ in the manner shown in Eq. (4) is essential in order that fluxes are generated both in the direction of the gradient, and in the directions normal to it. Retention of the scalar variance $\overline{\theta^2}$ is needed to incorporate the time scale of the scalar fluctuations. Of the remaining parameters in Eq. (3), the scalar fluxes themselves are excluded since that would render the model implicit in these quantities, while it is assumed that modeling the terms that are representative of diffusion and interactions with the fluctuating pressure will introduce terms similar to those already included in Eq. (4). Following usual practice, the dissipation term is neglected on the basis that it is small at high Reynolds number [1].

The procedure for modeling the scalar fluxes, a vector quantity, in terms of its vector and second-order tensor dependencies is well established [16]. The complete representation of $\overline{u_i\theta}$ produces many terms some of which will have zero coefficients while many others will be finite and their retention would render the model far too complex to be of practical use. However, simplifications can be made to render the model practical from a computational standpoint while retaining the essential dependencies required by the exact equation. Specifically, it can be assumed that terms that are quadratic in the mean velocity gradients or in the Reynolds stresses can be neglected on the basis that they represent a second-order effect that is not present in the original equation. With these simplifications, the following representation is obtained:

$$-\overline{u_i\theta} = \alpha_1\Theta_{,i} + \alpha_2\tau_{ij}\Theta_{,j} + \alpha_3(\tau_{ik}U_{k,j} + \tau_{jk}U_{k,i})\Theta_{,j} + \alpha_4 g_i \tag{5}$$

The $\alpha's$ in Eq. (5) contain combinations of the scalar quantities k, the turbulence kinetic energy, ϵ, the energy dissipation rate and $\overline{\theta^2}$, the scalar variance. Collectively, these serve the dual purposes of incorporating a characteristic time scale for turbulence (k/ϵ) and a characteristic thermal time scale ($\overline{\theta^2}/\epsilon_\theta$). Combinations of these parameters ensure that the terms of Eq. (5) are dimensionally consistent.

With the $\alpha's$ determined for each term, the proposed model takes the form:

$$-\overline{u_i\theta} = C_1\frac{k^2}{\epsilon}\frac{\partial\Theta}{\partial x_i} + C_2\frac{k}{\epsilon}\overline{u_iu_j}\frac{\partial\Theta}{\partial x_j} + C_3\frac{k^2}{\epsilon^2}\left(\overline{u_iu_k}\frac{\partial U_j}{\partial x_k} + \overline{u_ju_k}\frac{\partial U_i}{\partial x_k}\right)\frac{\partial\Theta}{\partial x_j} + C_4\frac{k}{\epsilon}\beta g_i\overline{\theta^2} \tag{6}$$

It is interesting to see that the first term of the model in Eq. (6) corresponds exactly to the familiar Fourier and Fick's laws: the imposition of a scalar gradient in the i-direction produces a scalar flux in the same direction. The remaining terms are also functions of the scalar gradient but in directions other than that of the fluxes. The implications here is that the imposition of a scalar gradient in the j- or k-directions can generate a flux in the i-direction irrespective of whether or not a gradient of the scalar exists in that direction. This aspect of the present model, which is supported by all experiments and Direct or Large Eddy Simulations, is not obtainable in the simpler models where the generation of a flux in a particular direction is only possible by the presence of a finite gradient of the scalar in the same direction.

2.2 Determination of model coefficients

The new model contains 4 coefficients that need to be determined. This is done here by reference to data from a study of homogeneous turbulence in neutrally and stably-stratified conditions. The study is that of Kaltenbach et al. [17] who performed Large-Eddy Simulations for the case of turbulence in the domain shown in Fig. 1. Gradients of velocity and temperature were applied as shown.

For the flow arrangement shown in Fig. 1, the model of Eq. (6) yields the following expressions for the scalar fluxes:

$$-\overline{u\theta} = C_2 \frac{k}{\epsilon} \overline{uw} \frac{\partial \Theta}{\partial z} + C_3 \frac{k^2}{\epsilon^2} \overline{w^2} \frac{\partial \Theta}{\partial z} \frac{\partial U}{\partial z} \tag{7}$$

$$-\overline{w\theta} = C_1 \frac{k^2}{\epsilon} \frac{\partial \Theta}{\partial z} + C_2 \frac{k}{\epsilon} \overline{w^2} \frac{\partial \Theta}{\partial z} + C_4 \frac{k}{\epsilon} \beta g \overline{\theta^2} \tag{8}$$

In assessing this model's performance, it is useful to compare its results with those from an alternative algebraic model. The model chosen for comparison is that of Gibson and Launder [6] which was shown to capture the effects of buoyancy on the atmospheric boundary layer. The model was obtained by approximating unknown correlations and then by assuming local equilibrium to reduce the differential equations to algebraic ones. This model's expressions for the scalar fluxes for the same conditions as for the LES of Kaltenbach et al. [17] are:

$$-\overline{u\theta} = \Phi_\theta \frac{k}{\epsilon} \overline{uw} \frac{\partial \Theta}{\partial z} + \Phi'_\theta \frac{k}{\epsilon} \overline{w\theta} \frac{\partial U}{\partial z} \tag{9}$$

$$-\overline{w\theta} = \Phi_{\theta 1} \frac{k}{\epsilon} \overline{w^2} \frac{\partial \Theta}{\partial z} + \Phi'_{\theta 1} \frac{k^2}{\epsilon^2} \beta g \overline{w\theta} \frac{\partial \Theta}{\partial z} \tag{10}$$

where the Φ's are model constants given in full in [6]. Like the model of Eq. (6), this model indicates that the gradients of mean velocity are present and enter into determination of the streamwise component only.

The Large-Eddy Simulations were performed for 5 values of the gradient Richardson number Ri:

$$Ri = \frac{\beta g \frac{d\Theta}{dz}}{\left(\frac{dU}{dz}\right)^2} \tag{11}$$

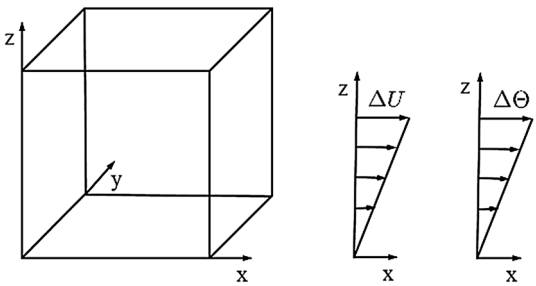

Fig. 1 Domain of Large Eddy Simulations

Table 1 Model coefficients as deduced from LES data of [17]

C_1	C_2	C_3	C_4
0.01	0.19	−0.06	−0.07

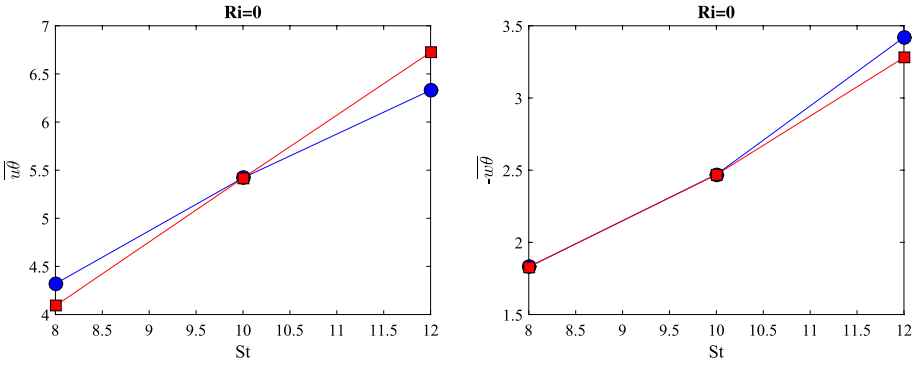

Fig. 2 Variation of heat fluxes with non-dimensional time St: ● Kaltenbach et al. [17], ■ Eq. (6)

where β is the constant volumetric expansion coefficient. This parameter was varied in the range 0 - 1. In each of these simulations, values of the scalar fluxes $\overline{u\theta}$ and $\overline{w\theta}$ were reported at 3 time intervals. For the case of $Ri = 0$, this yields 6 values that can serve to evaluate the coefficients C_1, C_2 and C_3. This makes the system of equations for the turbulent heat fluxes overdetermined though a unique set of values for these coefficients can be obtained by eliminating the sets of values that include negative C_1s or infinite coefficients. Determination of the value of C_4, the coefficient of the only term that explicitly depends on gravitational acceleration, was determined with reference to the LES results for Ri 0.13 and 0.5. The values thus obtained are listed in Table 1.

With the coefficients assigned the values of Table 1, the model of Eq. (6) predicts the evolution of the scalar fluxes for $Ri = 0$ as shown in Fig. 2. The horizontal axis is a non-dimensional time St $(= dU/dz\, t)$. It can be seen in Fig. 2 that for both $\overline{u\theta}$ and $\overline{w\theta}$ the relative error for the non buoyant case can be reduced to a tolerable number between 0 and 5% which was the goal of the new calibration.

3 Comparisons with LES and measurements

We first check the model's performance against data from two benchmark two-dimensional heated free shear flows namely the plane jet and the axisymmetric jet that are discharged into stagnant surroundings. A schematic of these flows is shown in Fig. 3 which defines the coordinates. In the experiments, the jets are allowed to develop in the streamwise direction until a self-similar state is attained wherein the flow properties, appropriately non-dimensionalized, become independent of the initial conditions. Also, the rates of spread of the shear layer $(d\delta_U/dx)$ and of the thermal layer $(d\delta_\Theta/dx)$ become constant. These flows, which are well documented by experiments, are ideal for the testing of models for the turbulent scalar fluxes since uncertainties regarding the specification of the initial conditions do not arise.

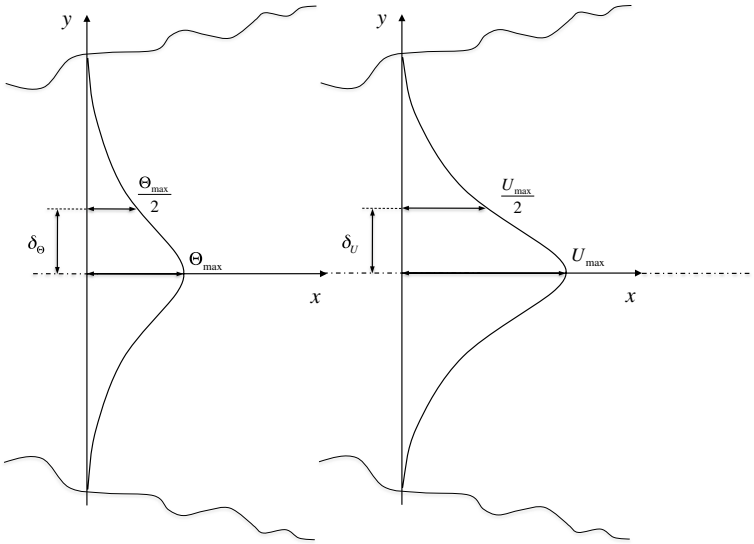

Fig. 3 Schematic of the free jet flows showing the coordinates system and the jet's velocity and thermal half widths

The computations were performed using the computer program EXPRESS [18] which solves the time-averaged forms of the equations governing the conservation of mass, momentum and thermal energy. In buoyant flows, the Boussinesq approximation is used wherein the density differences are ignored except where they appear in the source terms:

$$\frac{\partial U_i}{\partial x_i} = 0 \tag{12}$$

$$U_j \frac{\partial U_i}{\partial x_j} = \frac{\partial}{\partial x_j}\left(\nu \frac{\partial U_i}{\partial x_j} - \overline{u_i u_j}\right) - \frac{1}{\rho}\frac{\partial p}{\partial x_i} - g_i \beta \Delta\Theta \tag{13}$$

$$U_j \frac{\partial \Theta}{\partial x_j} = \frac{\partial}{\partial x_i}\left(\frac{\nu}{Pr}\frac{\partial \Theta}{\partial x_i} - \overline{u_i \theta}\right) \tag{14}$$

The governing equations were discretized by integration over finite volumes formed on a computational grid that adapts to maximize the spatial resolution of the expanding shear layers. Second-order accurate discretisation is employed for both streamwise and cross-stream directions using weighted average approximation for the former and central differencing for the latter. Typically, the simulations were carried out with 60 nodes that were evenly distributed in the cross-stream direction. Virtually identical results were obtained on grids utilizing 30 and 90 nodes. The solution was started from uniform velocity and temperature profiles and was advanced step by step in the direction of flow until the profiles of all the dependent variables became self similar. The size of the forward step was limited to 1% of the local width of the shear layer. At each streamwise location, iterations were performed until the absolute sum of the residuals for all the dependent variables fell to below 10^{-3}. In calculating the velocity field, the unknown Reynolds stresses were obtained from the solution of a complete Reynolds-stress transport model in which each of the three

normal-stress components and the non-zero component of shear stress were obtained from the solution of its own diffrential transport equation. These equations take the form:

$$\overbrace{U_k \frac{\partial \overline{u_i u_j}}{\partial x_k}}^{\text{Convection: } C_{ij}} = - \overbrace{\left(\overline{u_i u_k} \frac{\partial U_j}{\partial x_k} + \overline{u_j u_k} \frac{\partial U_i}{\partial x_k} \right)}^{\text{Production: } P_{ij}} \overbrace{- \beta \left(g_i \overline{u_j \theta} + g_j \overline{u_i \theta} \right)}^{\text{Production: } G_{ij}} - \overbrace{\frac{\partial}{\partial x_k} \left[\overline{u_i u_j u_k} + \frac{1}{\rho} (\overline{p' u_i} \delta_{jk} + \overline{p' u_j} \delta_{ik}) - \nu \frac{\partial \overline{u_i u_j}}{\partial x_k} \right]}^{\text{Diffusion: } D_{ij}} - \overbrace{2\nu \left(\overline{\frac{\partial u_i}{\partial x_k} \frac{\partial u_j}{\partial x_k}} \right)}^{\text{Dissipation: } \epsilon_{ij}} + \overbrace{\overline{\frac{p'}{\rho} \left(\frac{\partial u_i}{\partial x_j} + \frac{\partial u_j}{\partial x_i} \right)}}^{\text{Redistribution: } \Phi_{ij}} \tag{15}$$

In the above, P_{ij} and G_{ij} are the rates of production by shear and buoyancy. These terms are exact and in no need of modeling. The turbulent diffusion term is modeled as proposed by Daly and Harlow [19] i.e. by assuming that the diffusion of a component of the Reynolds stress tensor is proportional to its spatial gradient:

$$-\overline{u_i u_j u_k} = C_s \frac{k}{\epsilon} \overline{u_k u_l} \frac{\partial \overline{u_i u_j}}{\partial x_l} \tag{16}$$

The coefficient C_s is assigned its usual value of 0.22.

The pressure-strain correlations term ($\boldsymbol{\Phi}_{ij}$), whose role is to redistribute the turbulence energy amongst the three normal-stress components and to reduce the shear stresses, was modeled along the proposals of [20, 21]:

$$\begin{aligned} \boldsymbol{\Phi}_{ij} = & - (C_1 \epsilon + C_1^* P_k) b_{ij} + C_2 \epsilon \left(b_{ik} b_{kj} - \frac{1}{3} b_{kl} b_{kl} \delta_{ij} \right) \\ & + \left(C_3 - C_3^* II_b^{\frac{1}{2}} \right) k S_{ij} + C_4 k \left(b_{ik} S_{jk} + b_{jk} S_{ik} - \frac{2}{3} b_{kl} S_{kl} \delta_{ij} \right) \\ & + C_5 \left(G_{ij} - \frac{1}{3} \delta_{ij} G_{ii} \right) \end{aligned} \tag{17}$$

where $S_{ij} \left(= \frac{1}{2} \left(\frac{\partial U_i}{\partial x_j} + \frac{\partial U_j}{\partial x_i} \right) \right)$ is the mean rate of strain, $b_{ij} \left(= \overline{u_i u_j} / \overline{u_q u_q} - \frac{1}{3} \delta_{ij} \right)$ is the turbulence anisotropy and $II_b \left(= b_{ij} b_{ij} \right)$ is the second invariant of anisotropy. The model coefficients were assigned their usual values (Table 2).

To place the present model's results in some perspective, comparative predictions were obtained with a complete differential transport model for the scalar fluxes based on the solution of the modelled forms of Eq. (3). For the present two-dimensional flows, equations were solved for each of the fluxes $\overline{u\theta}$ and $\overline{w\theta}$. In these equations, the fluctuating pressure–scalar–gradient correlation term ($\pi_{i\theta}$) was modeled as the sum of two elements:

Table 2 Coefficients of the pressure-strain model [20]

C_1	C_1^*	C_2	C_3	C_3^*	C_4	C_5	$C_{\epsilon 1}$	$C_{\epsilon 2}$	C_ϵ
4.0	3.0	0	0.8	2.0	0.6	0.3	1.45	1.9	0.18

$$\pi_{i\theta} = \pi_{i\theta,1} + \pi_{i\theta,2} \tag{18}$$

the separate contributions arising respectively from purely turbulence interactions, and the interactions between the mean strain and fluctuating quantities. Following Monin [22] and Gibson and Launder [6], these contributions are modeled as:

$$\pi_{i\theta,1} = -C_{1\theta}\frac{\epsilon}{k}\overline{u_i\theta} \tag{19}$$

$$\pi_{i\theta,2} = -C_{2\theta}P_{i\theta,2} \tag{20}$$

The coefficients $C_{1\theta}$ and $C_{2\theta}$ were assigned the values of 2.85 and 0.55, respectively. These values were determined by reference to measurements of streamwise and cross-stream flux components in homogeneous shear flows [1].

Tables 3 and 4 list the predicted and measured rates of spread of the thermal layer ($d\delta_\Theta/dx$) for the heated plane jet and the axisymmetric jets, respectively. Also included in the tables are results obtained by using the differential model for the scalar fluxes as well as results from other algebraic models specifically those of Rogers et al. [25], Rubinstein and Barton [26], and the more familiar Fick's law with constant Prandtl number of 0.85. The Reynolds-stress transport model results were used to provide the necessary inputs to all the scalar-flux models considered thus differences in their performance are entirely due to their formulation. For the case of the plane jet, the experiments show some variance in the measured spreading rate which is to be expected considering the difficulty in attaining a self-preserving state for the thermal layer. The present model yields the closest correspondence with the data while the performance of Fick's law appears to be the least satisfactory. The same is the case for the axisymmetric flow though here all the models appear to underpredict the measured spreading rate.

The predicted and measured cross-stream profiles of mean temperature and the turbulent heat fluxes for the plane and the axisymmetric jets are presented in Fig. 4. For the mean temperature profile, the model of Eq. (6) shows a close agreement with the experimental results of Ramprian and Chanrasekhara [24] for a plane free jet and with Chen and Rodi [27] and Darisse et al. [28] for the axisymmetric jet. Regarding the streamwise heat flux component $\overline{u\theta}$, a quantity which is obtained as exactly zero with Fick's law, both the algebraic and the differential models, while yielding very similar results, yield

Table 3 Heated plane jet. Predicted and measured growth of thermal layer

	$d\delta_\Theta/dx$
Measurements [23, 24]	0.128, 0.140
Present model (Eq. 6)	0.131
Differential model	0.118
Rogers et al. [25]	0.125
Rubinstein and Barton [26]	0.117
Fick's Law (Eq. 1)	0.110

Table 4 Heated axisymmetric jet. Predicted and measured growth of thermal layer

	$d\delta_\Theta/dx$
Measurements [27]	0.11
Present model (Eq. 6)	0.102
Differential model	0.098
Rogers et al. [25]	0.064
Rubinstein and Barton [26]	0.091
Fick's Law (Eq. 1)	0.084

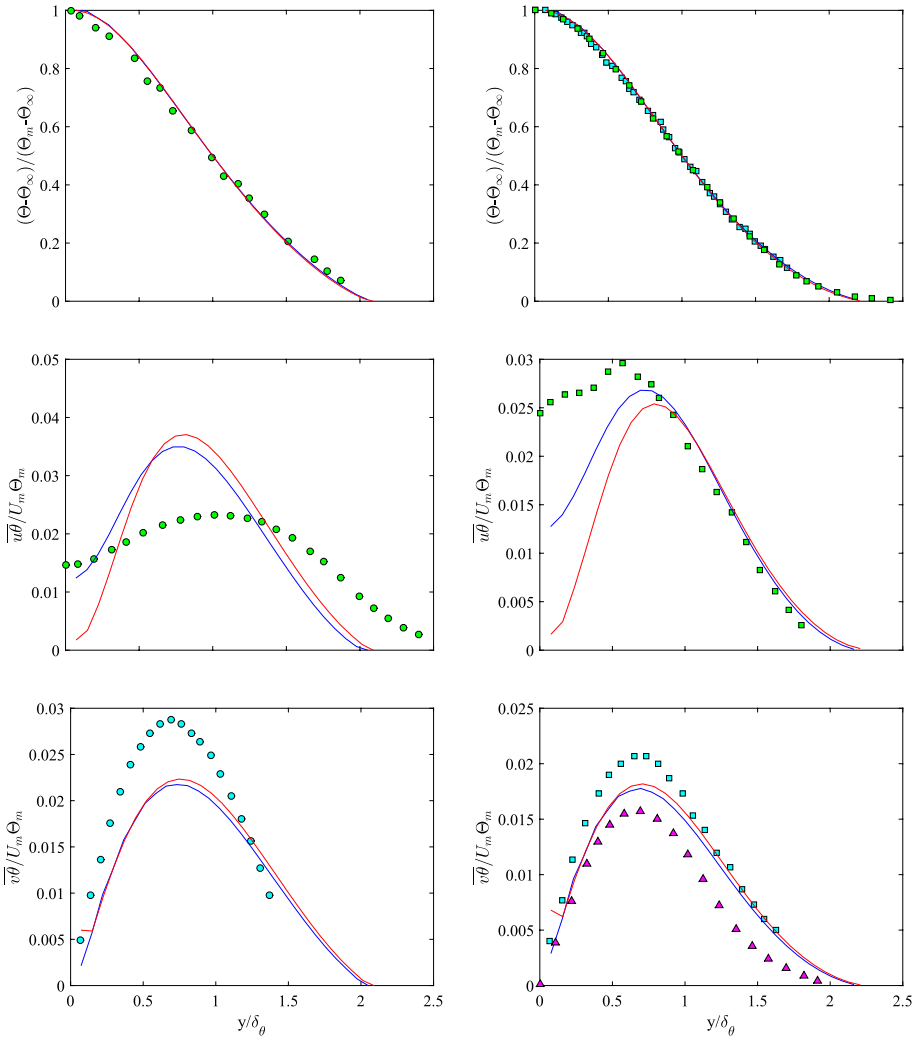

Fig. 4 Similarity profiles of mean temperature and turbulent heat fluxes for plane (left) and axisymmetric jet (right): ● van der Hegge Zijnen [23]; ● Ramaprian and Chandrasekhara [24]; ■ Chen and Rodi [27]; ■ Darisse et al. [28]; ▲ Chevray et al. [29]; —— Eq. (6); —– differential transport model

predictions that are at variance with the measurements of [24]. At the jet's axis, the algebraic model predicts a zero value for this flux since the gradients of temperature in both the streamwise and the cross-stream directions are zero. In contrast, the differential model predicts a finite value there which is maintained by the process of turbulent diffusion from regions away from the axis. The same behavior is apparent in the axisymmetric case where the two models succeed in reproducing the measured profile in the outer regions of the jet but appear to seriously underpredict the surprising high measured values in the inner region. With regards to the vertical heat fluxes $\overline{v\theta}$, the correspondence between the results of both the algebraic and the differential models and the experimental data is closer to the measurements than was the case for the streamwise component. For the plane jet, the results of the two models are almost indistinguishable everywhere in the flow, including near the centerline where this component of the heat flux goes to zero in both the predictions and the measurements of van der Hegge Zijnen [23]. For the axisymmetric jet, the models yield predictions that lie in between the measurements of Chen and Rodi [27] and Chevray et al. [29] with the differences between the two experiments providing a useful indication of the extent of uncertainty involved in the measurement of the thermal field in self-similar free shear flows.

An exacting test of the model's formulation is provided by examination of its behavior in conditions of very strong stable stratification. Linear stability theory [12, 13] indicates that turbulence is extinguished at values of the gradient Richardson number greater than a critical value Ri_{cr} in the range $0.20 - 0.25$. Grachev et al. [30], from spectral analysis of wind velocity and temperature fluctuations measurements in atmospheric turbulence, found that some small-scale turbulence can in fact persist for greater values of Ri, but that that turbulence is intermittent and decays rapidly with increasing stability. Within the constraints of a turbulence closure based on time-averaged equations, it is not possible to account for non-stationary effects, or for the fate of the small-scale, high-frequency fluctuations. Instead, it is assumed that a state of spectral equilibrium exists wherein the effects of buoyancy on the turbulence can be described solely in terms of long-time averaged fluxes of momentum and transported scalars, and their spatial gradients. In the present model, the response of the turbulent fluxes to stable stratification can be seen from inspection of the equation for the vertical scalar fluxes (Eq. 8). For stable stratification, the scalar gradients are positive and $\overline{w\theta}$ is negative. The gravitational term is itself negative (since if the positive vertical direction z is positive upwards as shown in Fig. 1, then $g_3 = -g_z$), and hence its effect is to diminish and eventually suppress turbulent mixing in the direction of the scalar gradient. In the LES of Kaltenbach et al. [17] for the temporal evolution of $\overline{w\theta}$, its value at Ri_{cr} falls by 6.2% of its value for neutral flow. This is accurately produced by the present model as can be seen in Fig. 5 and in Table 5 where the predicted values of the vertical heat flux $-\overline{w\theta}$ at Ri_{cr} are compared with the LES results.

Of further interest is the variation of the heat fluxes across a wide range of Ri. To demonstrate this, the LES results which were reported at three time intervals were averaged for each gradient Richardson number. Figures 6 and 7 present the development of $\overline{u\theta}$ and $-\overline{w\theta}$ with increasing Ri. The results of Eq. (6) are compared with Fourier's law and with the implicit model by Gibson and Launder [6]. For $\overline{u\theta}$, the effects of buoyancy enter mainly through the expected reduction in the correlations involving the vertical turbulent fluctuations i.e. $\overline{w^2}$ and $\overline{uw}$ since the contribution of the g_i term is identically zero for this component. Fourier's law predicts $\overline{u\theta}$ to be zero for all cases, since there is no temperature gradient in the streamwise direction. The model by Gibson and Launder overpredicts the neutrally-buoyant case by a significant margin but overall manages to reproduces the observed

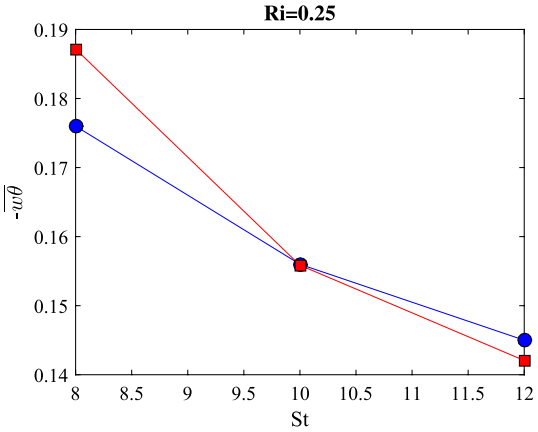

Fig. 5 Comparison with Kaltenbach data at $R_i = 0.25$: ■ Kaltenbach et al. [17], ● Eq. (6)

Table 5 LES and models results for the ratio $\left(\overline{w\theta}\right)_{Ri=Ri_{cr}} / \left(\overline{w\theta}\right)_{Ri=0}$

LES [17]	Present model (Eq. 6)	Gibson and Launder [6]
0.062	0.063	0.081

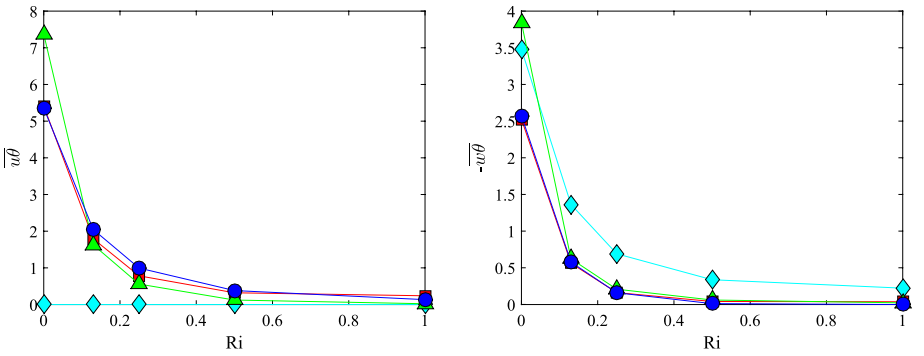

Fig. 6 Predicted variation of $-\overline{w\theta}$ with R_i: : ● Kaltenbach et al. [17], ■ Eq. 6, ◆ Fourier law (Eq. 1), ▲ Gibson and Launder [6]

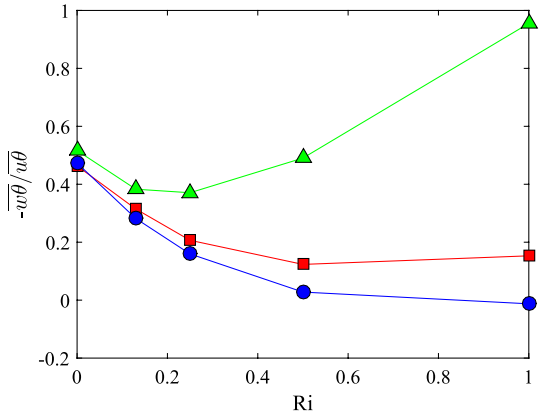

Fig. 7 Predicted variation of $-\overline{w\theta}/\overline{u\theta}$ with R_i. : ● Kaltenbach et al. [17], ■ Eq. (6), ▲ Gibson and Launder [6]

trend for increasing buoyancy. It slightly underpredicts $\overline{u\theta}$ for all buoyancy affected cases $Ri = 0.13 - 1$. The presented model shows very close alignment for the buoyancy free case at $Ri = 0$ and shows a good agreement with all buoyancy affected cases. It slightly underpredicts the flows with mild and moderate buoyancy $Ri = 0.13 - 0.25$. Severe buoyancy at $Ri = 0.5$ is predicted accurately whereas very severe buoyancy at $Ri = 1$ is slightly overpredicted by the presented model. For $-\overline{w\theta}$ both Fourier's law and the model by Gibson and Launder fail to obtain the correct level for $Ri = 0$. Fourier's law predicts a significantly higher $-\overline{w\theta}$ for all buoyancy affected cases $Ri = 0.13 - 1$ too. The implicit model by Gibson and Launder shows a good agreement for the buoyancy affected cases $Ri = 0.13 - 1$. In contrast, the model of Eq. (6) accurately predicts $-\overline{w\theta}$ at $Ri = 0$ and moreover shows close to perfect alignment at mild, moderate, severe and very severe buoyancy $Ri = 0.13 - 1$.

The ratio between the cross-stream and streamwise heat flux $\overline{w\theta}/\overline{u\theta}$ is considered to be an important assessment for the influence of buoyancy [6]. In strongly buoyant flows, it is expected to decrease distinctly and eventually trend against 0. Figure 7 presents the variation of the ratio $-\overline{w\theta}/\overline{u\theta}$ with Ri. This ratio is considered to be a good indicator of a scalar flux model's performance in buoyancy affected flows [6]. Fourier's law results are not plotted here since it would obtain this ratio as infinity. The model by Gibson and Launder produces generally good results for no and mild buoyancy $Ri = 0 - 0.13$ and gets the decreasing trend right initially. With increasing buoyancy $Ri = 0.25 - 1$ the error increases and a reverse trend can be observed with a strong increase of $-\overline{w\theta}/\overline{u\theta}$ for severe and very severe buoyancy $Ri = 0.5 - 1$. In contrast, the model of Eq. (6) manages to reproduce the qualitative trend of the strongly decreasing ratio. It shows good alignment for $Ri = 0 - 0.25$ and a stabilization from $Ri = 0.5$ to $Ri = 1$ which is similar to the LES data, though the LES continues to show a small decrease of $-\overline{w\theta}/\overline{u\theta}$ for high Ri.

It has already mentioned that models for the turbulent scalar fluxes that are based on the notion of an effective or eddy diffusivity (Eqs. 1 and 2) usually employ a constant Prandtl or Schmidt number in their formulation. By definition, this number is:

$$\sigma_t \equiv \frac{\overline{uw}/(dU/dz)}{\overline{w\theta}/(d\Theta/dz)} \tag{21}$$

It is evident from Eq. (21) that σ_t, far from being constant, will depend on Ri. This is borne out in Fig. 8 where the present model results for this parameter are compared with the LES results. Also plotted there are the experimental data by Grachev et al. [31] and the results of the implicit model of Gibson and Launder [6]. The data by Grachev et al., which were acquired during the Surface Heat Budget of the Arctic Ocean experiment (SHEBA), although showing considerable scatter, do support the trends evident in both the LES and the model results of an increase in σ_t with Ri. The Gibson and Launder model generally underpredicts this parameter even for neutrally-buoyant conditions where this model yields a value of σ_t of 0.40 compared to the value of 0.74 obtained with the present model and values in the range $0.7 - 0.9$ suggested in the literature [27]. We do not in this paper claim to provide a definitive statement regarding the behavior of σ_t with increasing stable stratification. Figure 8 merely shows that σ_t, when plotted against the gradient Richardson number Ri, tends to increase with increasing stability. Grachev et al. [31] and Anderson [32] explain that the trends shown in Fig. 8 may well be due to self-correlation since dU / dz and $d\Theta/dz$ appear in the definition of both σ_t and Ri. Moreover, Grachev et al. [33] point out that conclusions regarding the behavior of σ_t at high Ri may be influenced by Ri outliers i.e. high values of Ri formed from conditions that are actually near-neutral. While most theoretical studies (e.g. [34, 35]) do indeed predict an increasing σ_t with increasing stability,

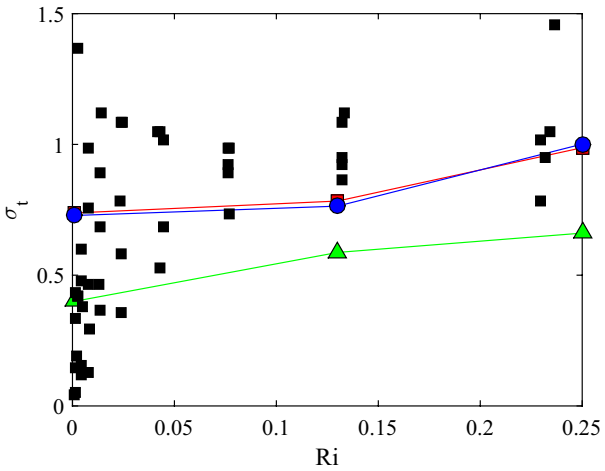

Fig. 8 Variation of the turbulent Prandtl number σ_t with R_i : ■ Grachev et al. [31], ● Kaltenbach et al. [17], ■ Eq. (6), ▲ Gibson and Launder [6]

the analysis of experimental data by Grachev et al. [31] show that σ_t, when plotted against the bulk Richardson number with which no variables are shared, actually decreases with increasing stability. The definition of the bulk Richardson number requires evaluation of differences in the potential temperature and the specific humidity between the surface and a reference level above it. Thus short of performing simulations of the atmospheric boundary layer in stable stratification that take into account the variation of the specific humidity, a task which is outside the scope of the present paper, it is not possible to state whether the present model would also show σ_t decreasing with increasing bulk Richardson number.

The final comparisons made in this study are with experimental data for vertical turbulent plumes. Here too both plane and axisymmetric flows are considered. In both the computations and experiments, the plumes were generated from a source of buoyancy with negligible momentum. The predicted and measured cross-stream profiles are compared in Fig. 9. For the plane buoyant plume, compared to the differential model, the present algebraic model yields overall better agreement with the measurements of Ramaprian and Chandrasekhara [24] especially for the vertical flux component which is the primary agency in determining the shape of the mean temperature profile. The algebraic model results for the streamwise component are less satisfactory in the inner region of the plume for the same reason as for the jets. For the axisymmetric plume, the predicted mean temperature profiles compare favorably with the measurements of George et al. [36]. For the turbulent fluxes, the trends of both the models results and the measurements of are generally similar to the plane plume case except, perhaps, for the maximum value of the streamwise flux component obtained in the measurements of Beuther et al. [37] which appears to greatly exceed the plane-plume value and is significantly underpredicted by both models.

4 Concluding remarks

The exact equations governing the conservation of the turbulent scalar fluxes in buoyant flows provided the basis for the development of the explicit algebraic model for these fluxes reported in this paper. The model correctly takes into account the dependence of these fluxes on the gradients of mean velocity and the transported scalar, and on

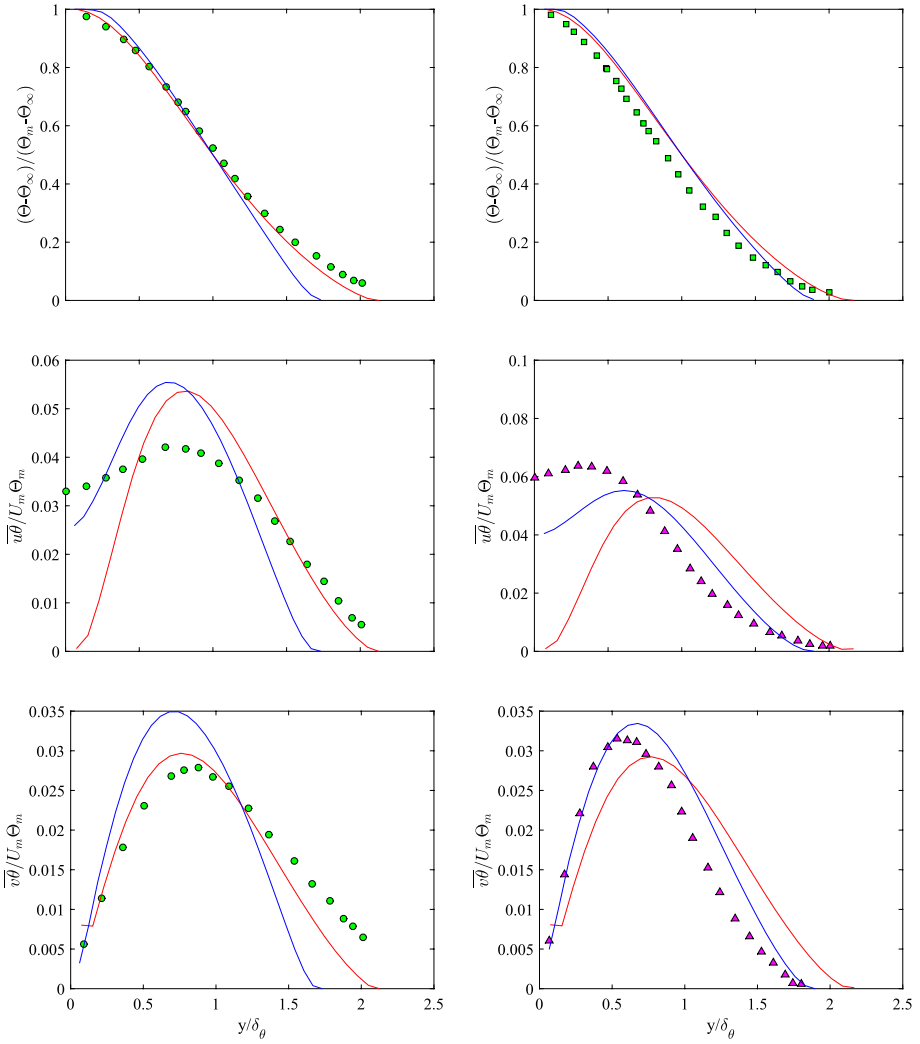

Fig. 9 Turbulent buoyant plumes. Predicted and measured profiles of temperature and turbulent heat fluxes for the plane (left) and axisymmetric (right) plumes: ● Ramaprian and Chandrasekhara [24]; ■ George et al. [36]; ▲ Beuther et al. [37]; —- present model (Eq. 6) ; —- differential transport model

the gravitational acceleration. A number of coefficients are involved and these were assigned constant values deduced from Large-Eddy Simulations of homogeneous turbulence with uniform gradients of mean velocity and temperature. Comparisons with data from neutrally-stratified two-dimensional free shear flows, namely the heated plane and the axisymmetric jets discharged into stagnant surroundings, show that the coefficients deduced from the LES data are quite appropriate in that they closely reproduce the cross-stream profiles of mean temperature and both streamwise and cross-stream heat fluxes. With regards to buoyant flows, the model properly reproduces the variation of these components of the scalar fluxes with the gradient Richardson number and, also,

the temporal evolution of the vertical component at the critical value of this parameter. The turbulent Prandtl number, which is assumed to be constant in many models, is predicted to vary with the gradient Richardson number in accordance with experimental observations and numerical simulations. Comparisons with measurements of the temperature field in plane and axisymmetric buoyant plumes show that the present model results are on par with those obtained with a more elaborate and computationally more demanding model requiring the solution of non-linear differential equations for the turbulent fluxes. Work is currently in progress to assess the model's performance in stably-stratified wall-bounded flows for which detailed results from LES and DNS (e.g. [38, 39]) are available for this purpose.

Acknowledgements Y. Jooß gratefully acknowledges the financial support provided by the Hermann-Reissner-Foundation to support his stay at the University of California, Davis.

References

1. Malin MR, Younis BA (1990) Calculation of turbulent buoyant plumes with a Reynolds stress and heat flux transport closure. Int J Heat Mass Transf 33:2247–2264
2. Violeau D (2009) Explicit algebraic Reynolds stresses and scalar fluxes for density-stratified shear flows. Phys Fluids 21(3):035103. https://doi.org/10.1063/1.3081552
3. Martynenko OG, Korovkin VN (1994) Flow and heat transfer in round vertical buoyant jets. Int J Heat Mass Transf 37:51–58
4. Younis BA, Speziale CG, Clark TT (2005) A rational model for the turbulent scalar fluxes. Proc R Soc 461:575–594
5. Rodi W (1976) A new algebraic relation for calculating the Reynolds stresses. Z Angew Math Mech 56:219–221
6. Gibson MM, Launder BE (1978) Ground effects on pressure fluctuations in the atmospheric boundary layer. J Fluid Mech 86:491–511
7. So RMC, Vimala P, Jin LH, Zhao CY (2002) Accounting for buoyancy effects in the explicit algebraic model: homogeneous turbulent shear flows. Theor Comput Fluid Dyn 15:283–302
8. Vanpouille D, Aupoix B, Laroche E (2015) Development of an explicit algebraic turbulence model for buoyant flows—Part 2: model development and validation. Int J Heat Fluid Flow 53:195–209
9. Lazeroms WMJ, Brethouwer G, Wallin S, Johansson AV (2013) An explicit algebraic Reynolds-stress and scalar-flux model for stably stratified flows. J. Fluid Mech. 723:91–125
10. Pope S (1975) A more general effective-viscosity hypothesis. J Fluid Mech 72:331–340
11. Lazeroms WMJ, Brethouwer G, Wallin S, Johansson AV (2015) Efficient treatment of the nonlinear features in algebraic Reynolds-stress and heat-flux models for stratified and convective flows. Int J Heat Fluid Flow 53:15–28
12. Miles J (1961) On the stability of heterogeneous shear flows. J Fluid Mech 10:496–508
13. Howard L (1961) Note on a paper of John W. Miles. J Fluid Mech 10:509–512
14. Mellor GL (1975) A comparative study of curved flow and density-stratified flow. J Atmos Sci 32:1278–1282
15. Gibson MM (1978) An algebraic stress and heat-flux model for turbulent shear flow with streamline curvature. Int J Heat Mass Transf 21:1609–1617
16. Smith GF (1994) Constitutive equations for anisotropic and isotropic materials. North-Holland, Amsterdam
17. Kaltenbach HJ, Gerz T, Schumann U (1994) Large-eddy simulation of homogeneous turbulence and diffusion in stably stratified shear flow. J Fluid Mech 280:1–40
18. Younis BA (1996) EXPRESS: Accelerated Parabolic Reynolds Stress Solver. Hydraulics Section Report HDBAY1, City University, London
19. Daly BJ, Harlow FH (1970) Transport equations of turbulence. Phys Fluids 13:2634–2649
20. Dafalias YF, Younis BA (2009) Objective model for the fluctuating pressure-strain-rate correlations. J Eng Mech 135:1006–1014. https://doi.org/10.1061/(ASCE)EM.1943-7889.0000014

21. Malin MR, Younis BA (1990) Calculation of turbulent buoyant plumes with a Reynolds stress and heat flux transport closure. Int J Heat Mass Transf 33:2247–2264
22. Monin AS (1965) On the symmetry properties of turbulence in the surface layer of air. Isv Atmos Ocean Phys 1:45–54
23. van der Hegge Zijnen BG (1958) Measurement of the velocity distribution in a plane turbulent jet of air; measurement of the distribution of heat and matter in a plane turbulent jet of air. Appl Sci Res A 7:256–292
24. Ramaprian BR, Chandrasekhara MS (1983) Study of vertical plane jets and plumes. IIHR Report no. 257, University of Iowa, USA
25. Rogers MM, Mansour NN, Reynolds WC (1989) An algebraic model for the turbulent flux of a passive scalar. J Fluid Mech 203:77–101
26. Rubinstein R, Barton J (1991) Renormalization group analysis of anisotropic diffusion in turbulent shear flows. Phys Fluids A 3:415–421
27. Chen CJ, Rodi W (1980) Vertical turbulent buoyant jets: a review of experimental data. Pergamon, Oxford
28. Darisse A, Lemay J, Benassa A (2013) Investigation of passive scalar mixing in a turbulent free jet using simultaneous LDV and cold wire measurements. Int J Heat Fluid Flow 44:284–292
29. Chevray R, Tutu NK (1978) Intermittency and preferential transport of heat in a round jet. J Fluid Mech 44:133–160
30. Grachev AA, Andreas EL, Fairall CW, Guest PS, Persson POG (2013) The critical Richardson number and limits of applicability of local similarity theory in the stable boundary layer. Bound-Layer Meteorol 147:51–82. https://doi.org/10.1007/s10546-012-9771-0
31. Grachev AA, Andreas EL, Fairall CW, Guest pS, Persson POG (2007) On the turbulent Prandtl number in the stable atmospheric boundary layer. Bound-Layer Meteorol 125:329–341
32. Anderson PS (2009) Measurement of Prandtl number as a function of Richardson number avoiding self-correlation. Bound-Layer Meteorol 131:345–362
33. Grachev AA, Andreas EL, Fairall CW, Guest PS, Persson POG (2012) Outlier problem in evaluating similarity functions in the stable atmospheric boundary layer. Bound-Layer Meteorol 144:137–155. https://doi.org/10.1007/s10546-012-9714-9
34. Galperin B, Sukoriansky S, Anderson PS (2007) On the critical Richardson number in stably stratified turbulence. Atmos Sci Lett 8:65–69
35. Li D, Katul GG, Zilitinkevich SS (2015) Revisiting the turbulent Prandtl number in an idealized atmospheric surface layer. J Atmos Sci 72:2394–2410. https://doi.org/10.1175/JAS-D-14-0335.1
36. George WK, Alpert RL, Taminini F (1977) Turbulence measurements in an axisymmetric buoyant plume. Int J Heat Mass Transf 20:1145–1154
37. Beuther SP, Capp RL, George WK (1979) Momentum and temperature balance measurements in an axisymmetric turbulent plume. ASME Publication 79-HT-42
38. Armenio V, Sarkar S (2002) An investigation of stably stratified turbulent channel flow using large-eddy simulation. J Fluid Mech 459:1–42
39. Garcia-Villalba M, del Alamo JC (2011) Turbulence modification by stable stratification in channel flow. Phys Fluids 23:045104